Cellulose (2024) 31:2713–2727
https://doi.org/10.1007/s10570-024-05786-z

ORIGINAL RESEARCH

Influence on the structure and the molecular mobility of cellulose–diamine complexes studied by a multiscale experimental approach

Agustín Rios de Anda · Axel Ettori · Yoshiharu Nishiyama · Karim Mazeau · Caroll Vergelati · Laurent Heux

Received: 15 May 2023 / Accepted: 29 January 2024 / Published online: 2 March 2024
© The Author(s), under exclusive licence to Springer Nature B.V. 2024

Abstract In this paper, the influence of diamines on the intrinsic structure and molecular mobility of cellulosic complexes is discussed. Cellulose was pre-swollen by ethylenediamine then put in contact with a series of aliphatic diamines at a stoechiometric ratio. These materials were then characterized by Wide Angle X-Ray diffraction (WAXS) and solid-state ^{13}C NMR spectroscopy. It was observed by WAXS that diamines are able to swell cellulose along the (010) crystallographic plane and are able to modify unit cell angle γ of cellulose monoclinic structure. Moreover according to their periodicity, ordered- or disordered-phases structures were identified in such cellulosic complexes by Cross Polarization - Magic Angle Spinning (*CP-MAS*) ^{13}C NMR spectroscpy. Two-dimensional Wide-line Separation (*2D WISE*) and T_1 relaxation time ^{13}C NMR spectroscopy experiments showed that complexes do exhibit molecular motions between 23 and 90°C. Modulated Differential Scanning Calorymetry (*MDSC*) further showed the presence of two glass transition temperatures T_g, which were attributed, in combination with the ^{13}C NMR spectroscopy observations through a multiscale approach, to relaxation motions internal to the diamines chemical structure and to the motion of cellulose–diamine planes respectively.

Keywords Cellulose · Cellulosic complexes · Molecular relaxations · Solid-state NMR spectroscopy · X-ray diffraction

This article is part of a collection of articles in honor of Dr. Henri Chanzy on the occasion of his 90th birthday. The article was not finished in time to be bound with the rest of the papers in the Special Issue #13, September, 2023

A. R. de Anda (✉) · A. Ettori · Y. Nishiyama · K. Mazeau · L. Heux
CERMAV - Centre de Recherche sur les Macromolécules Végétales - UPR 5301, BP53 - 38041, Grenoble Cedex 9, France
e-mail: agustin.rios-de-anda@u-pec.fr

L. Heux
e-mail: laurent.heux@cermav.cnrs.fr

Present Address:
A. R. de Anda
Université Paris Est Créteil, CNRS, ICMPE, UMR 7182, 2 rue Henri Dunant, 94320 Thiais, France

C. Vergelati
Solvay in Axel'One, 85 rue des frères Perret, 69192 Saint Fons Cedex, France

Introduction

Cellulose, a polysaccharide, is the most abundant natural macromolecule. The interest and the research conducted on this polymer has spanned for over almost a century. As a naturally-sourced biodegradable material exhibiting outstanding mechanical properties it has found applicative uses such as in structural, biomedical, technical and packaging applications (Diddens et al. 2008; Gericke et al.

2013; Reddy et al. 2013). On the other hand, because of the strong inter- and intra-chain hydrogen bonds present in its structure (Mazeau 2005; Mazeau and Heux 2003; Pinkert et al. 2009), cellulose cannot be dissolved by standard solvents nor be processed by thermal methods as its glass transition temperature is higher than its decomposition temperature (Calahorra et al. 1989), resulting in high-pressure and solvent-induced processing methods (Schroeter and Felix 2005; Wang et al. 2012a; Wu et al. 2015). This remains a major issue, since cellulose cannot be processed as a "standard" thermoplastic polymer. As such, physical and chemical modifications have been carried in cellulose to render this macromolecule processable, yielding bulk cellulose-derivate materials. As of now however, processing of native or pure cellulose remains still an open subject for research.

A proposed means to possibly overcome this is by physically swelling cellulose by integrating molecules within its structure. In order to do so, the targeted molecules should be able to strongly interact with cellulose and be able to disturb the H-bond network of this material. Indeed the strength of an amine-alcohol H bond is of *ca.* 30 kJ/mol whereas that of an alcohol-alcohol bond is of *ca.* 20 kJ/mol (Gill and Noll 1972; Hopmann 1974; Jorgensen and Swenson 1985; Klotz and Franzen 1962). Primary amines are then a good candidate as target molecules since they can interact through their $-NH_2$ functions with the -OH moieties of cellulose and thus disrupt the H-bond network to some extent. Several studies on amine-cellulose complexes have been conducted with ethylenediamine (*EDA*) as a target molecule aimed to swell cellulose (Ishikura 2011; Nishiyama et al. 2010; Numata et al. 2003; Segal and Loeb 1960; Su et al. 2011; Wada et al. 2009, 2008). These studies have shown that *EDA* is effectively able to disrupt the H-bond network of cellulose and it is able to modify its crystalline arrangement, i.e. cellulose I becomes cellulose III after complexation and elimination of *EDA*. Moreover, studies on cellulosic complexes with several types of amines (such as mono-, di-, and trifunctional as well as primary, secondary or tertiary amines, hydrazine, and ammonia have been carried out in the literature (Chundawat et al. 2011; Creely and Wade 1975; Creely et al. 1978, 1959; Davis et al. 1943; Segal 1964; Segal and Eggerton 1964; Wada et al. 2011; Wang et al. 2012b). Such investigations so far have dealt with the feasibility of obtaining such complexes as well as studying the influence of these amines on the crystalline structure of cellulose, specifically on the crystallographic planes, as well as the evolution of such structures with temperature. It has been observed that such molecules are capable of modyfing the inner structure of cellulose, provoking a disruption of its crystallographic planes.

In this work we seek to deepen the study of the influence of primary diamines on the intrinsic structure and the molecular mobility of cellulosic complexes that has been developed in the literature. To do so we chose a series of diamine aliphatic molecules having an increasing size ranging from 2 to 12 carbons, so as to have a well-defined periodicity. Moreover, we considered such molecules as they can form two H bonds per molecule at their extremities, thus giving the possibility of creating “physical” bridges between cellulose chains in the complex. Moreover, having the same nature as EDA, we would expect these molecules to strongly bond to cellulose and induce a similar effect on its structure. We firstly characterized the structure of the obtained complexes by X-ray diffraction (Chanzy 2011; Nishiyama 2009; Nishiyama et al. 2008, 2002, 2003; Parthasarathi et al. 2011; Wada et al. 2001) and solid-state ^{13}C *CP-MAS* NMR spectroscopy (Earl and VanderHart 1981, 1980; Heux et al. 1999; Kono and Numata 2004; Kono et al. 2002; Larsson et al. 1999, 1997; Mori et al. 2012; Numata et al. 2003; VanderHart and Atalla 1984; Wada et al. 2009; Wickholm et al. 1998; Wormald et al. 1996), two techniques that have been used extensively to study cellulose. Afterwards we investigated the molecular mobility within these materials at several temperatures by *2D WISE* and T_1 relaxation time solid-state ^{13}C NMR spectroscopy measurements. These two techniques have been proven very efficient in characterizing the molecular dynamics of synthetic polymers (Schmidt-Rohr and Spiess 2005) and we have

adapted the experimental conditions in this study to examine our cellulose–diamine complexes.

Experiemental

Materials and cellulose–diamine complexes processing

We considered Flax cellulose fibers as the source material for our measurements. Flax cellulose is partially crystalline (30%) and provides with a regular structure that is capable of being characterized by X-Ray diffraction. To obtain the studied cellulose–diamine complex materials, this cellulose was physically complexed with a series of diamine molecules. The molecular structure of such diamines is shown in Fig. 1. These diamines are called herein *NMDA*, except for ethylene diamine (*EDA*), where *N* stands for the number of carbons between NH2 groups in the molecule and *MDA* stands for methylenediamine. All diamines were purchased from Sigma Aldrich with a purity <99%. Figure 1 also shows the chemical structure for a cellulose monomer (French 2017) with highlighted carbons of interest for the structural characterization.

Table 1 Physicochemical properties of the studied diamine molecules (Hodgman 1962)

Diamine	T_m (°C)	M (g/mol)	$d_{H_2N-R-NH_2}$ (nm)
EDA	8	60.1	0.377
3MDA	−12	74.1	0.493
4MDA	27.5	88.2	0.620
5MDA	11.8	102.2	0.749
6MDA	39–42	116.2	0.868
7MDA	26–30	130.2	0.988
8MDA	50–52	144.3	1.117
12MDA	67–69	200.4	1.620

The physicochemical properties of these diamines such as their melting temperature T_m, molar mass M, and distance between $-NH_2$ groups ($d_{H_2N-R-NH_2}$) within each diamine molecule are listed in Table 1. $d_{H_2N-R-NH_2}$ was obtained by modeling the extended conformation of each molecule with the ACD/Labs ChemSketch Version 2015.2.5 freeware. Molecules were traced in this software and then a modeling

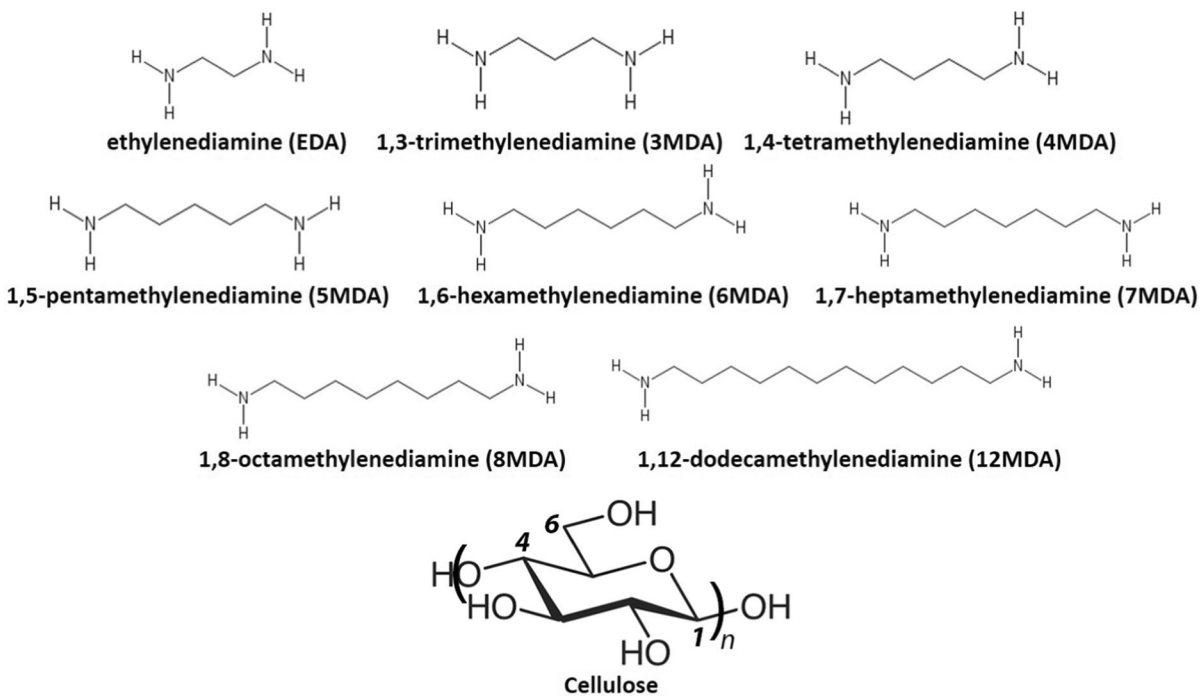

Fig. 1 Chemical structure and adopted nomenclature for the studied diamine molecules and for a cellulose monomer (French 2017)

and equilibrating of the molecule in 3D was undertaken before determining the distance between NH_2 groups for each molecule. This quantity $d_{H_2N-R-NH_2}$ was considered to define the molecular size of a given diamine.

To obtain the studied complexes, cellulose was firstly dried under vacuum for 1 h at 60°C then it was pre-swollen by putting it in contact with ethylene diamine (*EDA*) for one hour at room temperature. The excess of *EDA* was eliminated by evaporating this molecule under vacuum overnight at room temperature. Afterwards the cellulose-*EDA* complex was put in contact with a given diamine introduced at molar stoechiometric proportions, i.e. 1 diamine molecule per glucose moiety. The whole was put in a round-bottom flask and heated at a temperature 20°C higher than the melting temperature of the given diamine. The complexation was done thus at the liquid state for the targeted diamine without the presence of any solvent. An inert atmosphere was needed to avoid carbonation of the amine and was obtained by allowing a flux of dry N_2 into the flask. The complexation time was fixed at 24 h, by which time the given diamine had displaced the bonded *EDA* and complexed with the cellulose. Gravimetric measurements confirmed that each *EDA* molecule was subsequently substituted by one diamine molecule.

X-ray diffraction characterization

To characterize the inner structure of the complexes, Wide Angle X-Ray diffraction measurements were carried out at our laboratory with a Philips PW3830 X-Ray Generator. The sample was placed 22 cm from the X-Ray source and the detection film was placed 15 cm from the sample. X-Ray beams had a KCuα filter of 1.54Å and their energy was set at 30 kV and 20 mA. Acquisition time was set at one hour per sample. The diffraction patterns were recorded on photographic films, which were later scanned and analyzed with ImageJ.

^{13}C solid state NMR spectroscopy characterization

In order to characterize the complexes' relaxation dynamics at a molecular level, we conducted different characterization techniques using solid-state ^{13}C NMR spectroscopy measurements. All of these experiments were conducted in a Bruker Avance III 400 NMR spectrometer equipped with a 4 mm MAS DVT probe and a MAS II module. The resonance frequency for ^{1}H was of 400.130 MHz and that for ^{13}C was of 100.613 MHz. Samples were introduced into 4 mm ZrO_2 with *KelF* caps. For all samples the ^{1}H excitation time was set at 5 s, the $\pi/2$ pulse time was of 3.5μs and the ^{1}H-^{13}C cross-polarization contact time was of 1ms. In the case of samples tested at temperatures higher than room temperature, the probe was stabilized at the set temperature for an hour with the rotor spinning.

Cross polarization - magic angle spinning experiments

CP-MAS (Cross Polarization - Magic Angle Spinning) measurements were conducted at room temperature and at high temperatures between 70 and 100°C. Such experiments were done so as to observe an eventual chemical shifting on the cellulose and the diamine carbons due to an increase of molecular mobility as a function of the temperature. Such experiments were done with a rotating speed of 12 kHz.

2D WISE experiments

2D WISE (Two-dimensional Wide-line Separation) experiments, which allowed to identify and quantify the rigid and mobile fractions in cellulose–diamine complexes, were undertaken. The principle of the measurement is the following: the cross polarization from ^{1}H to ^{13}C is delayed compared to a standard CP-MAS experiment. This delay has as a consequence that the protons located in rigid parts will relax very quickly and thus will not be able to induce a cross polarization to the adjacent carbons. However the mobile protons will slowly relax and be able to transfer their magnetization to adjacent carbons. This will create a difference of transfer between rigid and mobile regions in the sample, which will yield

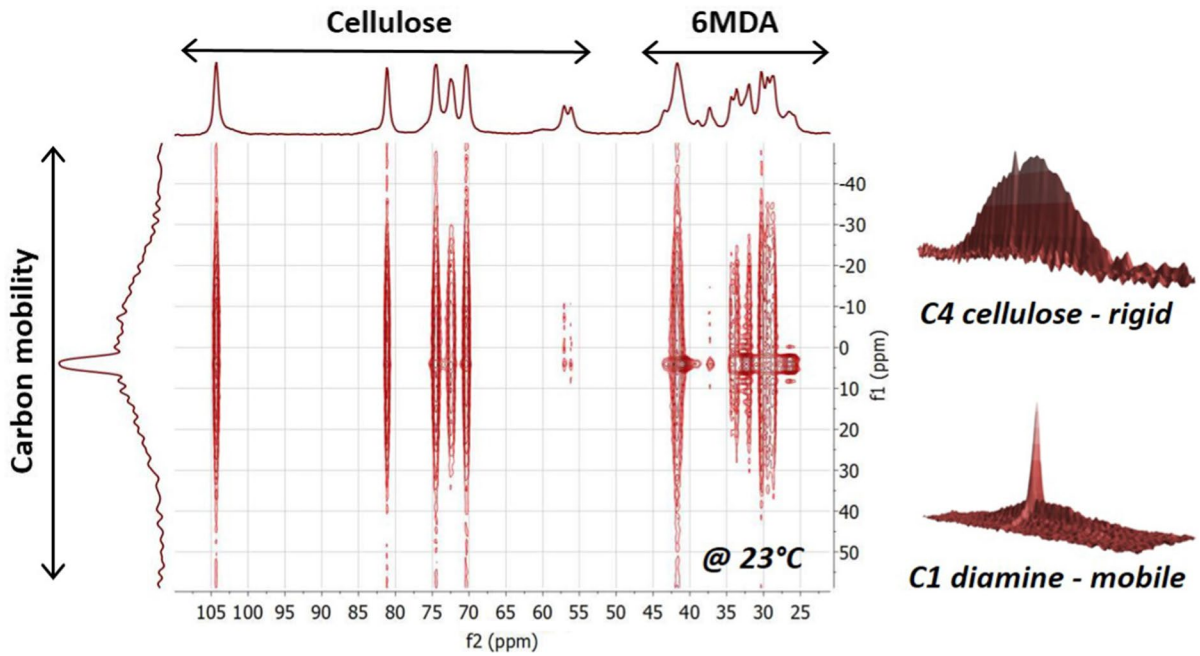

Fig. 2 *2D WISE* results for the Cellulose-6MDA complex studied at 23°C where the horizontal projection corresponds to the ^{13}C spectrum and the vertical projection corresponds to the sum of the rigid and mobile fractions of the whole complex

different relaxation patterns. In the case of rigid zones, the pattern will be a large peak, whereas the signature of a mobile fraction will be a sharp peak (Schmidt-Rohr and Spiess 2005). Measurements were conducted on Celullose-*6MDA* and Cellulose-*7MDA* complexes at 23, 75, and 90°C with a rotating speed of 6 kHz and a cross-polarization delay contact time of 1 s. As an example, Fig. 2 shows the *2D WISE* results for the Cellulose-6MDA complex characterized at 23°C.

T_1 *relaxation experiments*

Finally T_1 traverse relaxation times experiments were carried out to complement the study on the molecular mobility of the cellulose diamine complexes. For these experiments a cross-polarization between ^1H and ^{13}C is followed by a $\pi/2$ pulse and then by a delay time before the acquisition is made (Schmidt-Rohr and Spiess 2005). Measurements were conducted on Celullose-*6MDA* and Cellulose-*7MDA* complexes at 23, 75, and 90°C with a rotating speed of 12 kHz and delay times of 0.00001, 0.2, 0.4, 0.8, 1.6, 3.2, 6.4, and 12.8 s.

Modulated DSC characterization

Modulated DSC measurements were conducted on a TA Q2000 in the temperature - modulated mode. cellulose–diamine complex samples were put in non-hermetic aluminum pans and heated at 3°C/min with a temperature modulation of 2°C every 60 s from 25 to 150°C. This method has proven to allow the observation of glass transition phenomena in polymers for which it is difficult to measure this temperature (Pang et al. 1999; Rios de Anda et al. 2016, 2014, 2011). Three measurements per complex were done with the T_g for each sample being taken at the inflection point of the heat capacity step in the Reversing Heat Flow signal.

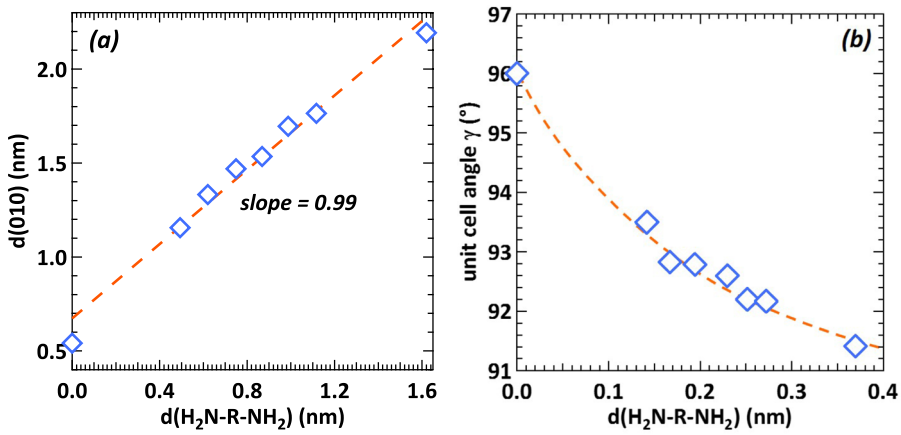

Fig. 3 **a** Distance of the $d(010)$ crystallographic plane of cellulose and **b** unit cell angle γ plotted as a function of the distance between $-NH_2$ groups in a diamine molecule $d_{H_2N-R-NH_2}$. The dashed lines are guides for the eyes

Results and discussion

Structural characterization by x-ray diffraction

The inner structure of cellulose–diamine complexes was studied by X-Ray diffraction at room temperature. From the diffraction patterns, cell parameter values corresponding to the $d(010)$ plane of cellulose were extracted. It is known in the literature that this is the plane affected by the presence of diamines (Chundawat et al. 2011; Creely and Wade 1975; Creely et al. 1978, 1959; Davis et al. 1943; Ishikura 2011; Nishiyama et al. 2010; Numata et al. 2003; Segal 1964; Segal and Eggerton 1964; Segal and Loeb 1960; Su et al. 2011; Wada et al. 2009, 2008, 2011; Wang et al. 2012b). The numerical value of the cell parameter for the $d(010)$ plane was then plotted in Fig. 3a as a function of the distance between $-NH_2$ groups in a diamine molecule $d_{H_2N-R-NH_2}$. Figure 3a does not include the values for EDA, as this molecule has a larger stoichiometric ratio (i.e. 2 molecules of EDA per −OH function in cellulose) than the rest of the diamines (i.e. 1 −NH2 of diamine per −OH function in cellulose).

It is shown in Fig. 3a that for the cellulose–diamine complexes, the increase of the cell parameter in the $d(010)$ plane varies linearly with $d_{H_2N-R-NH_2}$. Moreover it is seen that the slope has the value of the unity, which would mean that the increase in the cell parameter of the $d(010)$ plane is directly proportional to the diamine size and the molar stoichiometry of the complexes. To further this analysis, from the diffraction patterns, the unit cell angle γ for each complex was determined from Eq. 1. Indeed, as the unit cell of cellulose I crystals is monoclinic, thus γ is different from 90° (Wada et al. 2008). The obtained values of γ are plotted in Fig. 3b as a function of $d_{H_2N-R-NH_2}$ for each cellulose-amine complex.

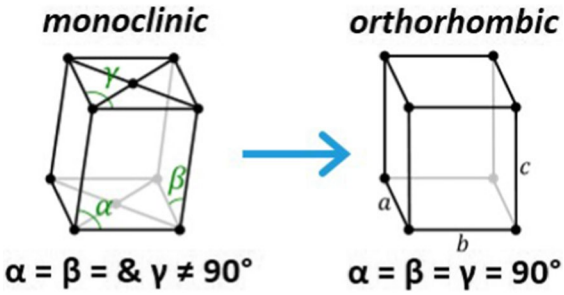

Fig. 4 Schematic representation of monoclinic and orthorombic cristalline unit cells

$$\gamma = 180° - \left(\frac{d_{1\bar{1}0}^2}{d_{100}^2 + d_{010}^2 + 2d_{100}d_{010}} \right) \quad (1)$$

Figure 3b shows that the value of γ decreases with $d_{H_2N-R-NH_2}$, i.e. an increasing diamine size, and leans towards 90°. This would mean that the crystalline cell unit tends to evolve from a monoclinic towards an orthorhombic structure when diamines are present in cellulose as shown schematically in Fig. 4.

It is important to note that the orthorhombic structure is more symmetric than the monoclinic cell. This

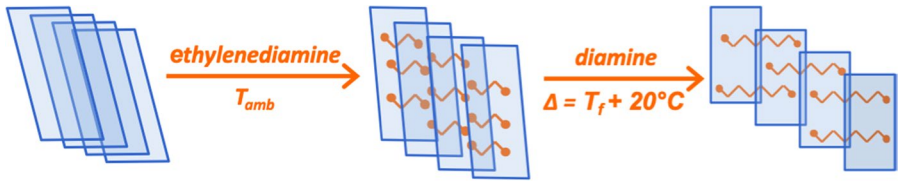

Fig. 5 Schematic representation of the modification of the *d*(010) plane of cellulose due to diamine swelling

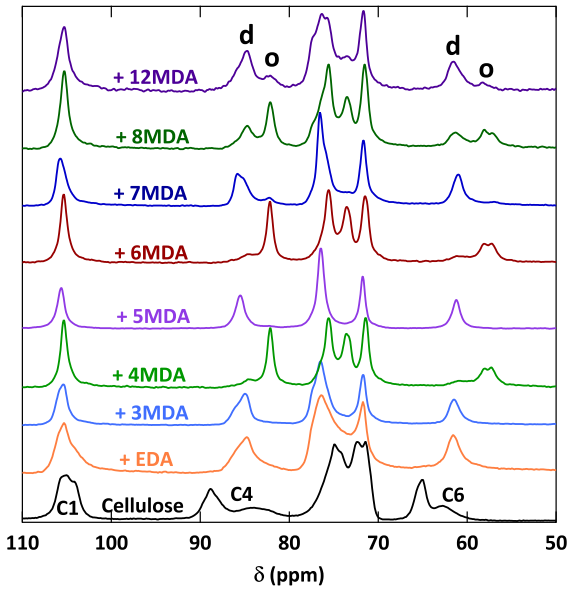

Fig. 6 ^{13}C CP-MAS NMR spectra zoomed on the cellulose chemical shifts obtained at room temperature for neat cellulose and for the studied cellulose–diamine complexes

confirms the results observed in the literature, showing that diamines are able to effectively modify the intercalary planes of cellulose, prompting the modification of its crystalline structure, as shown schematically in Fig. 5.

Structural characterization by ^{13}C CP-MAS NMR spectroscopy

The obtained cellulose–diamine complexes were then characterized by ^{13}C CP-MAS NMR spectroscopy at room temperature. Special interest was paid to the cellulose chemical shift region. The obtained spectra for such complexes and for neat cellulose are shown in Fig. 6.

A focus on the chemical shifts corresponding to the *C4* and *C6* carbons in cellulose was made. The

Table 2 Ordered phase ratio calculated from ^{13}C CP-MAS NMR spectroscopy in Fig. 6 for each cellulose–diamine complex

Cellulose complex	Ordered phase (%)
Neat	–
+ EDA	0
+ 3MDA	0
+ 4MDA	90
+ 5MDA	0
+ 6MDA	87
+ 7MDA	9
+ 8MDA	64
+ 12MDA	22

NMR spectra plotted in Fig. 6 show that in presence of diamines, the peaks corresponding to the *C4* (90 ppm) and *C6* (65 ppm) carbons are deshielded, and that the chemical shifts of the remaining cellulose carbons (76-70 ppm) are also modified. This is a signature of the effective complexation of diamines on cellulose (Wormald et al. 1996). Moreover it is observed that two peaks are observed for the *C4* and *C6* carbons depending on the diamine structure. These peaks are believed to correspond to disordered and ordered phases within the nner chemical structure of cellulose complexes. Herein, the signals for *C4* were considered to determine the disorderd and ordered phases of cellulose–diamine complexes. The peak corresponding to the disordered phase appears at around 85 ppm whereas the ordered peak signal appears at around 82 ppm. This has been already determined by Wormald et al. (1996) where they observed the same chemical shifts in the *C4* and *C6* cellulose carbons for samples having undergone water immersion-drying and mechanical tension cycles. In this work, a pattern is observed and is the following: for even-numbered diamines both orderered and disordered peaks are

observed, with the ordered intensity being larger and when the size of the diamine increases, the ordered peak intensity decreases. On the other hand, for odd-numbered diamines, the disordered peak intensity is the largest and that when the diamine size increases, an ordered peak appears and the intensity of the disordered signal decreases. To summarize and quantify these observations, the ordered phase ratio for each complex was calculated by integrating the organized and disorganized peak surfaces. These values are shown in Table 2.

To explain this periodicity, the proposed hypothesis is based on what has been observed for even- and odd-numbered polymers such as polyamides (Koham 1995; Puiggalí et al. 1998) as well as on liquid crystals and organic molecules organizing through H-bonds (Badea et al. 2006; Marčelja 1974; Mizuno et al. 2002; Thalladi et al. 2000; Uno et al. 2008). For instance, it is well known that even-numbered polyamides have higher glass transition and melting temperatures as well as a larger crystalline fraction than those of odd-numbered polyamides. This is due to the fact that because of the space arrangement of polyamide chains, even-numbered polymers can form a > C = O I I I HN– hydrogen bond for every amide in the structure whereas this number is cut by half for odd-numbered polyamides. Such similar effects are observed in liquid crystals and organic molecules bearing H bonding groups. In this case, even-numbered diamines yield a preponderant ordered phase could be possible because these molecules are favored to H-bond with two cellulose chains at a time without modifying their canonical geometrical orientation. Odd-numbered diamines however will have to modify this structure and twist in space onto less favorable orientations in order to form two H bonds at once, giving a more disordered structure. This is schematically shown in Fig. 7 where it is shown that an even-numbered diamine is able to bond twice to two glucose moieties in the same plane, whereas an odd-numbered diamine is only able to bond once in the same plane. This 2D representation was obtained by modeling such complexes with the ACD/Labs ChemSketch Version 2015.2.5 freeware.

Molecular mobility by ^{13}C NMR spectroscopy

2D WISE ^{13}C NMR spectroscopy experiments were then conducted on the Cellulose-6MDA and Cellulose-*7MDA* complexes at 23, 75 and 90°C. To study the evolution of the molecular mobility of the complexes, the C4 and C6 carbons of cellulose (i.e. Figure 1) and the carbons immediately adjacent to the $-NH_2$ functions for *6MDA* and *7MDA* were chosen. Their molecular mobility was extracted from their individual 1D rigid-mobile projection given by *2D WISE* ^{13}C NMR spectroscopy experiments. An example of such projections for Cellulose C4 carbon and

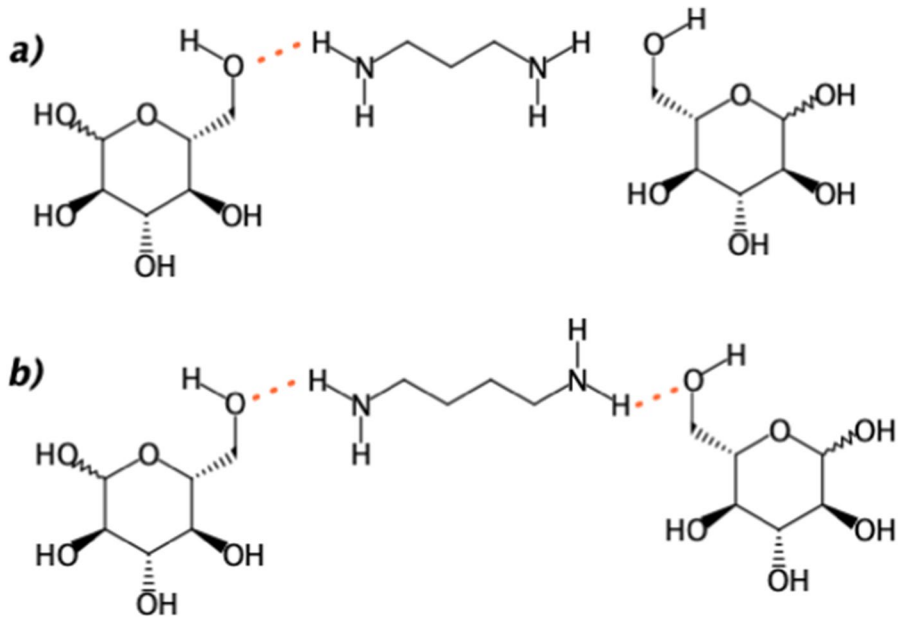

Fig. 7 Schematic representation of cellulose–diamine complexes showing that **a** odd-numbered diamines are only able to bond once to two glucose moieties in the same plane **b** whereas even-numbered diamines are able to bond twice in the same plane. This 2D representation was obtained by modeling such complexes with the ACD/Labs ChemSketch Version 2015.2.5 freeware

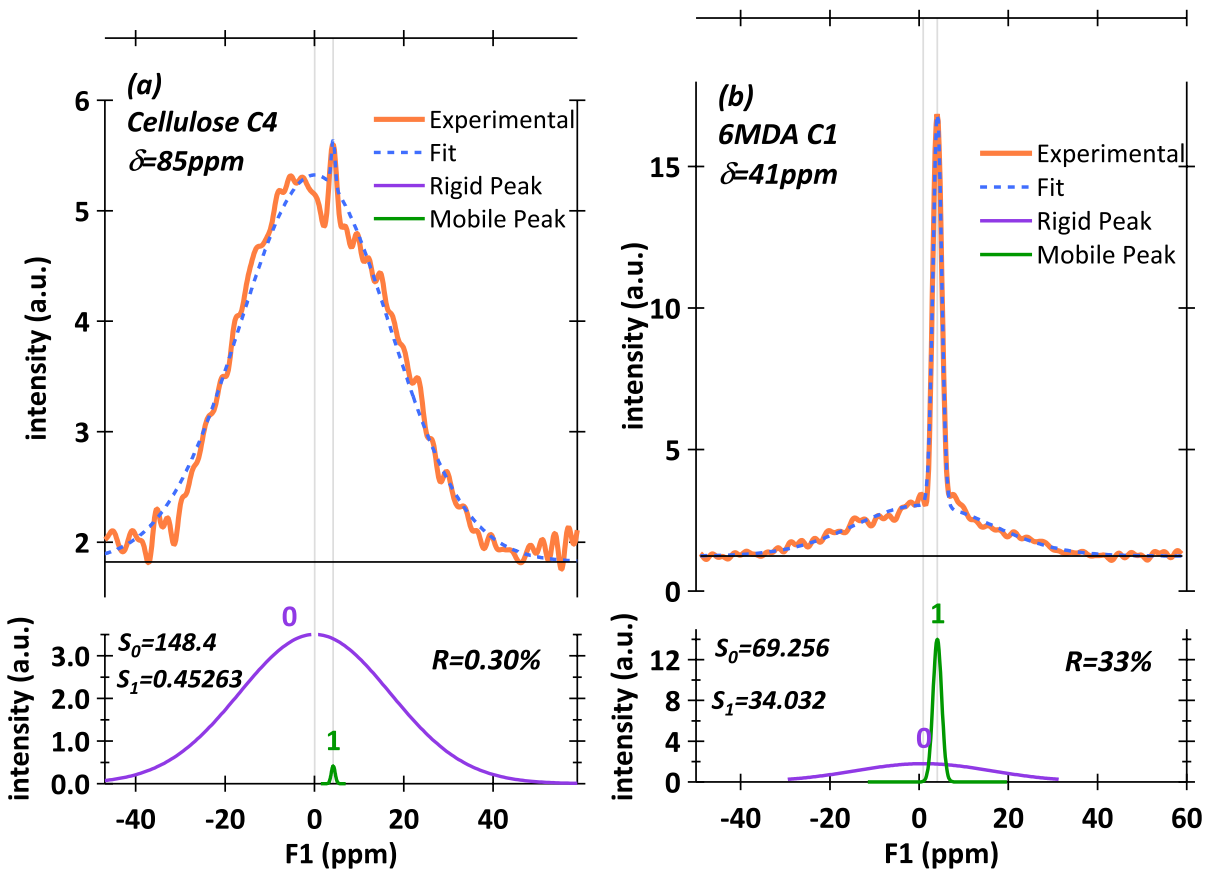

Fig. 8 ^{13}C 1D rigid-mobile projection obtained by *2D WISE* ^{13}C NMR spectroscopy experiments for **a** the C4 carbon of cellulose (i.e. Fig. 1) and **b** the carbons immediately adjacent to the $-NH_2$ functions for *6MDA*. The projections are deconvoluted into rigid (large peak) and mobile (sharp peak) components fitted by the IgorPro Version 6.32 software

Table 3 Mobile fractions for selected cellulose carbons (C1, C4, C6, i.e. Figure 1) and for the carbons immediately adjacent to the $-NH_2$ functions in *6MDA* and *7MDA*, for these cellulose–diamine complexes calculated from *2D WISE* ^{13}C NMR spectroscopy experiments at 23, 75 and 90°C

	Carbon	δ (ppm)	Cellulose-6MDA			Cellulose-7MDA		
			23°C	75°C	90°C	23°C	75°C	90°C
Cellulose	C1	104	0.3	1.0	0.6	1.0	1.1	1.8
	C4	85	0.3	0.4	0.4	0.0	0.7	0.0
	C6	57	1.0	0.9	0.6	2.1	2.6	3.0
Diamine	Adjacent to $-NH_2$	42	33.0	43.3	55.2	33.8	36.9	40.1

the carbons immediately adjacent to the $-NH_2$ functions of 6MDA is given in Fig. 8.

Figure 8 further shows the undertaken data analysis. The 1D projections were deconvoluted into two Gaussian peaks fitted by the IgorPro Version 6.32 software. The proportion of rigid and mobile fractions was then calculated by dividing the surface of the mobile peak over the total surface for both the rigid and mobile peaks. These results are listed in Table 3.

Table 3 shows that the selected cellulose carbons in both complexes remain mainly rigid even at 90°C. It is important to mention that because samples are

spun at 6 kHz, it might be possible that if there is a molecular relaxation corresponding to the movements of cellulose within the complex, it would be higher than 90°C and that this temperature would be shifted of at least 25°C towards higher temperatures, *ca.* 6°C per frequency decade according to the time-temperature equivalence principle (Hallary et al. 2010). In the case of diamines, it is seen in Table 3 that at room temperature these molecules have a non-negligible mobility fraction, which would mean that inner motions within diamines have already relaxed, i.e. that their proper glass transition temperature T_g has been reached and passed over. To explain this phenomenon let us liken the studied cellulose–diamine complexes to high density polyethylene (HDPE). Indeed, the studied diamines could be considered as oligomeric polyethylene (i.e. $-(CH_2-CH_2)_n$) chains. HDPE has a high crystalline fraction (ca. 80%), so PE chains in the amorphous phase are highly constrained. The glass transition temperature of this phase increases from -120°C for an amorphous PE to between -20 and 0°C for HDPE, as has been observed by DMA (Sewda and Maiti 2013). In the case of the studied cellulose–diamine complexes, as *2D WISE* ^{13}C NMR spectroscopy measurements are carried out well over this range of temperature, it would be likely that a fraction of diamines has indeed relaxed. Furthermore, Table 3 shows that the mobile fraction of amine increases with temperature. This would mean that the diamines within the complex are somehow mobile at temperatures between 23 and 90°C and that a higher amount of amines relaxes with increasing temperature.

To complete these experiments, T_1 ^{13}C NMR spectroscopy relaxation measurements were conducted on the cellulose-*6MDA* complex. The evolution of the sample magnetization, and thus the evolution of its molecular mobility, by choosing the C4 and C6 carbons of cellulose (i.e. Figure 1) and the carbons immediately adjacent to the $-NH_2$ functions for *6MDA* was considered. All samples magnetization were normalized (i.e. M_0) to that obtained for measurements with a delay acquisition time of 0.00001s. An example of the evolution of the chosen carbons normalized magnetization M/M_0 for the

Table 4 τ_1, τ_2, and τ_3 relaxation regime times obtained for the C4 and C6 of Cellulose (i.e. Figure 1) and for the carbons immediately adjacent to the $-NH_2$ functions in *6MDA* in the Cellulose-*6MDA* complex obtained by T_1 ^{13}C NMR spectroscopy experiments at 23, 75 and 90°C

Relaxation regime	Temperature (°C)	T_1 relaxation times (s)		
		Cellulose Carbons		Diamine Carbon
		C4	C6	Adjacent to $-NH_2$
τ_1	23	0.450	0.667	0.386
	75	0.368	0.560	0.308
	90	0.366	0.540	0.282
τ_2	23	1480	750	5.9
	75	400	7.3	3.2
	90	49	3.7	2.5
τ_3	23	–	–	38.4
	75	–	17.6	8.9
	90	–	6.4	–

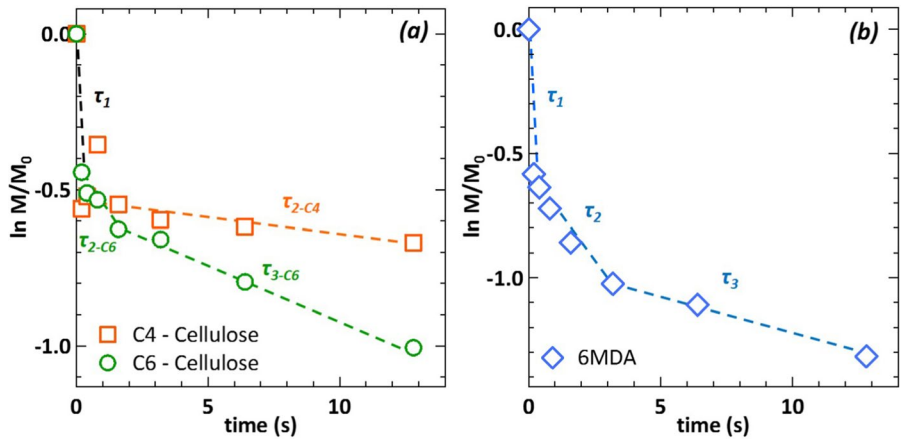

Fig. 9 Normalized magnetization relaxation as a function of the delay obtained by T_1 ^{13}C NMR spectroscopy experiments time for **a** the C4 carbon of cellulose (i.e. Fig. 1) and **b** the carbons immediately adjacent to the $-NH_2$ functions for *6MDA*. Dashed lines are exponential fits allowing the extraction of τ_1, τ_2, and τ_3 relaxation times listed in Table 4

cellulose-*6MDA* complex characterized at 23°C as a function of the delay acquisition time is shown in Fig. 9.

Figure 9 shows three mayor relaxation time regimes for the diamine carbons and the C6 of cellulose, and two regimes for the C4 of cellulose. The first regime τ_1 has a very short relaxation time (i.e. less than a second) for both the diamine and cellulose and can be attributed to fast local motions withing the carbons. The second τ_2 and third τ_3 regimes have relaxation times varying from the tens of second (diamines and C6 of cellulose) to the hundreds of seconds (cellulose). These relaxation regimes are a signature of molecular motions within the complex (i.e. relaxation times of the diamines and cellulose) and can be indirectly linked to the mobility observed by *2D WISE* ^{13}C NMR spectroscopy measurements. The numerical values of τ_1, τ_2, and τ_3 were obtained by fitting each regime with an exponential function. These values, obtained at 23, 75, and 90°C, are listed in Table 4.

From Table 4, it can be observed for the carbons in *6MDA* that their τ_2 and τ_3 relaxation times diminish, and even disappear when the temperature rises. This is a clear indication that the molecular mobility of this diamine increases with temperature. Then, for cellulose, it is seen in Table 4 that the C4 carbon has a relatively long τ_2 relaxation time which remains constant with increasing temperature. This means that this carbon remains rigid in the range of considered temperatures. In the case of the C6 carbon, it is observed that τ_2 and τ_3 relaxation times, albeit larger than those of the diamine, diminish with increasing temperature. This may be due to the fact that H bonds between diamines and cellulose are formed mostly through this carbon. As vicinal diamines relax with increasing temperature, so would this carbon, which is also the most mobile of all cellulose carbons. This could be thus considered as a signature of the beginning of cellulose molecular relaxations activated by the presence of diamines and by a rise in temperature.

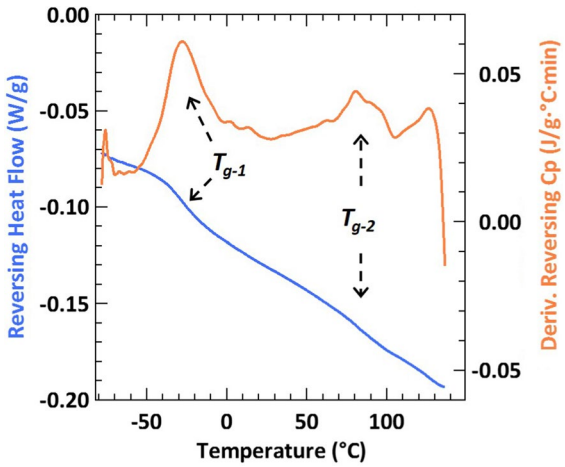

Fig. 10 Reversing Heat Flow and Derivative of the Reversing Thermal Capacity C_P with temperature as a function of temperature obtained by MDSC for the cellulose-6MDA sample highlighting the presence of two transition temperatures T_g. Data is plotted with the EXO UP convention

Molecular mobility by MDSC

Finally, the molecular mobility at a macroscopic scale was assessed by Modulated DSC for cellulose–diamine complexes containing either *EDA*, *6MDA*, and *7MDA*. By analyzing the Reversing Heat Flow (Rios de Anda et al. 2016, 2014, 2011) and the derivative of the Reversing Thermal Capacity C_P with temperature (Pang et al. 1999) it was possible to dissociate the phenomena responding in phase with the modulated ramp (i.e. glass transition temperature T_g) from kinetic phenomena (i.e. melting, chemical reactions, solvent evaporation, oxidation, etc.). Glass transitions appear as steps on the Reversing Heat Flow and as peaks on the derivative of the Reversing Thermal Capacity C_P with temperature. Figure 10 shows a thermogram plotting both signals as a function of temperature for the cellulose-*6MDA* complex.

As shown in Fig. 10, two transition temperatures T_g were observed for the three studied complexes, their values are listed in Table 5.

Table 5 shows that T_{g-1} (herein named sub-zero T_g) seems to be independent of the diamine as regards 6MDA and 7MDA and that its temperature range for the three cellulose–diamine complexes is similar

Table 5 Glass transition temperatures T_g measured by Modulated DSC for selected cellulose–diamine complexes

Cellulose complex	T_{g-1} (°C)	T_{g-2} (°C)
Neat	-	-
+ EDA	0.1 ± 0.4	93.1 ± 4.1
+ 6MDA	-24.5 ± 3.2	83.8 ± 2.8
+ 7MDA	-27.1 ± 5.1	78.1 ± 0.7

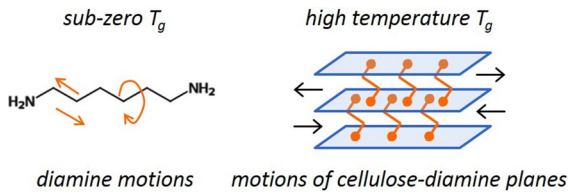

Fig. 11 Proposed origin of the two glass transition temperatures T_g observed by Modulated DSC in combination with molecular mobility phenomena observed by *2D WISE* and T_1 ^{13}C NMR spectroscopy measurements

to that of the T_g measured for HDPE as mentioned in section 3.3, i.e. between -20 and 0°C (Sewda and Maiti 2013). T_{g-2} (herein called high temperature T_g) on the other hand seems to depend on the diamine length. Indeed, the larger the diamine in the complex, the lower T_{g-2}.

From these measurements, and in combination with the results observed by *2D WISE* and T_1 ^{13}C NMR spectroscopy through a multiscale approach, the following origin of these two glass transition temperatures is proposed:

- The sub-zero T_g would correspond to the relaxation motions internal to the chemical structures of the diamines that are activated at temperatures between -20 and 0°C as in the case of HDPE (Sewda and Maiti 2013), as diamines in the studied complexes are highly constrained by celullose chains.
- The high temperature T_g would correspond to the motion of cellulose–diamine planes, which can be linked to the fact that at temperatures of 70°C and above, a rise in molecular mobility in diamines and on the *C6* cellulose carbon was observed by ^{13}C NMR spectroscopy measurements. Moreover, this tempertaure is related to the diamine size in each complex. Indeed, the larger the diamine, the easier it would be to induce the motion of cellulose–diamine planes as cellulose chains are further separated from each other, thus requiring less energy (*ergo* temperature) to induce these motions.

To summarize this analysis, Fig. 11 shows schematically the molecular origin of both glass transition temperatures.

Conclusion

In this work, the influence of a series of diamines in the structure and the molecular mobility of cellulosic complexes was investigated. It was shown that the presence of such molecules has a notable influence on cellulose structure. For instance, X Ray diffraction experiments demonstrated that the (010) crystallographic plane of the monoclinic unit cell increases almost linearly with the size of diamines, and the unit cell angle γ diminishes and tends towards 90° when the diamine molecular size increases, leading to a crystal structure variation from a monoclinic to an orthorhombic cell. Moreover, solid-state ^{13}C *CP-MAS* NMR spectroscopy showed that complexes with even-numbered diamines induce mostly an "ordered" structure phase in cellulose whereas odd-numbered diamines yield a majoritarian "disordered" structure. Afterwards, *2D WISE* and T_1 relaxation time solid-state ^{13}C NMR spectroscopy experiments revealed that between 23 and 90°C molecular movements can be observed and characterized within the cellulose–diamine complexes. Finally, Modulated DSC evidenced two glass transition temperatures in cellulose–diamine complexes. Through a multiscale approach combining the results from this technique to those obtained by ^{13}C NMR spectroscopy, the sub-zero T_g was attributed to relaxation motions internal to the diamines chemical structure, while the high temperature T_g was attributed correspond to the motion of cellulose–diamine planes.

Acknowledgements Not applicable.

Author contributions ARA and AE conducted the experiments, YN, KM, CV and LH supervised the project. All authors contributed to the writing and editing of the manuscript.

Funding This work was funded by, and author A. Ríos de Anda received research support from Solvay.

Date availability Not applicable.

Declarations

Conflict of interest Not applicable.

Ethical approval and consent to participate Not applicable.

Consent for publication All authors have given consent for publication.

References

Badea E, Della Gatta G, D'Angelo D, Brunetti B, Rečková Z (2006) Odd-even effect in melting properties of 12 alkane-α, ω-diamides. J Chem Thermodyn 38(12):1546–1552. https://doi.org/10.1016/j.jct.2006.04.004

Calahorra M, Cortazar M, Eguiazábal J, Guzmán G (1989) Thermogravimetric analysis of cellulose: effect of the molecular weight on thermal decomposition. J Appl Polym Sci 37(12):3305–3314. https://doi.org/10.1002/app.1989.070371203

Chanzy H (2011) The continuing debate over the structure of cellulose: historical perspective and outlook. Cellulose 18(4):853–856. https://doi.org/10.1007/s10570-011-9547-6

Chundawat SP, Bellesia G, Uppugundla N, da Costa Sousa L, Gao D, Cheh AM, Agarwal UP, Bianchetti CM, Phillips GN Jr, Langan P et al (2011) Restructuring the crystalline cellulose hydrogen bond network enhances its depolymerization rate. J Am Chem Soc 133(29):11163–11174. https://doi.org/10.1021/ja2011115

Creely J, Wade R (1975) Complexes of diamines with cellulose: Study of symmetrical and unsymmetrical terminal group effects. Text Res J 45(3):240–246. https://doi.org/10.1177/004051757504500309

Creely J, Wade R, French A (1978) X-ray diffraction, thermal, and physical studies of complexes of cellulose with secondary diamines. Text Res J 48(1):37–43. https://doi.org/10.1177/004051757804800106

Creely JJ, Segal L, Loeb L (1959) An x-ray study of new cellulose complexes with diamines containing three, five, six, seven, and eight carbon atoms. J Polym Sci 36(130):205–214. https://doi.org/10.1002/pol.1959.1203613017

Davis W, Barry A, Peterson F, King A (1943) X-ray studies of reactions of cellulose in non-aqueous systems. ii. interaction of cellulose and primary amines1. J Am Chem Soc 65(7):1294–1299. https://doi.org/10.1021/ja01247a012

Diddens I, Murphy B, Krisch M, Müller M (2008) Anisotropic elastic properties of cellulose measured using inelastic x-ray scattering. Macromolecules 41(24):9755–9759. https://doi.org/10.1021/ma801796u

Earl WL, VanderHart D (1981) Observations by high-resolution carbon-13 nuclear magnetic resonance of cellulose i related to morphology and crystal structure. Macromolecules 14(3):570–574. https://doi.org/10.1021/ma50004a023

Earl WL, VanderHart DL (1980) High resolution, magic angle sampling spinning carbon-13 nmr of solid cellulose i. J Am Chem Soc 102(9):3251–3252. https://doi.org/10.1021/ja00529a064

French AD (2017) Glucose, not cellobiose, is the repeating unit of cellulose and why that is important. Cellulose 24(11):4605–4609. https://doi.org/10.1007/s10570-017-1450-3

Gericke M, Trygg J, Fardim P (2013) Functional cellulose beads: preparation, characterization, and applications. Chem Rev 113(7):4812–4836. https://doi.org/10.1021/cr300242j

Gill S, Noll L (1972) Calorimetric study of association of diketopiperazine in water. J Phys Chem 76(21):3065–3068. https://doi.org/10.1021/j100665a027

Hallary JL, Lauprêtre F, Monnerie L (eds) (2010) Polymer Materials. Macroscopic Properties and Molecular Interpetrations. John Wiley & Sons, Hoboken

Heux L, Dinand E, Vignon M (1999) Structural aspects in ultrathin cellulose microfibrils followed by 13c cp-mas nmr. Carbohydr Polym 40(2):115–124. https://doi.org/10.1016/S0144-8617(99)00051-X

Hodgman C (ed) (1962) CRC Handbook of Chemistry and Physics, 44th edn. CRC Press, Cleveland

Hopmann RF (1974) Chemical relaxation as a mechanistic probe of hydrogen bonding. thermodynamics and kinetics of lactam isoassociation in nonpolar solvents. J Phys Chem 78(23):2341–2348. https://doi.org/10.1021/j150671a009

Ishikura Y (2011) Changes of wood properties treated with aqueous amine solution, bending tests and x-ray analysis of wood after amine treatment. J Mater Sci 46(11):3785–3791. https://doi.org/10.1007/s10853-011-5292-3

Jorgensen WL, Swenson CJ (1985) Optimized intermolecular potential functions for amides and peptides. hydration of amides. J Am Chem Soc 107(6):1489–1496. https://doi.org/10.1021/ja00292a007

Klotz IM, Franzen JS (1962) Hydrogen bonds between model peptide groups in solution. J Am Chem Soc 84(18):3461–3466. https://doi.org/10.1021/ja00877a009

Koham M (ed) (1995) Nylon Plastics Handbook. Carl Hanser Verlag, Munich

Kono H, Numata Y (2004) Two-dimensional spin-exchange solid-state nmr study of the crystal structure of cellulose ii. Polymer 45(13):4541–4547. https://doi.org/10.1016/j.polymer.2004.04.025

Kono H, Yunoki S, Shikano T, Fujiwara M, Erata T, Takai M (2002) Cp/mas 13c nmr study of cellulose and cellulose derivatives. 1. complete assignment of the cp/mas 13c nmr spectrum of the native cellulose. J Am Chem Soc 124(25):7506–7511. https://doi.org/10.1021/ja010704o

Larsson PT, Hult EL, Wickholm K, Pettersson E, Iversen T (1999) Cp/mas 13c-nmr spectroscopy applied to structure and interaction studies on cellulose i. Solid State Nucl Magn Reson 15(1):31–40. https://doi.org/10.1016/S0926-2040(99)00044-2

Larsson PT, Wickholm K, Iversen T (1997) A cp/mas13c nmr investigation of molecular ordering in celluloses. Carbohydr Res 302(1–2):19–25. https://doi.org/10.1016/S0008-6215(97)00130-4

Marčelja S (1974) Chain ordering in liquid crystals. i. even-odd effect. J Chem Phys 60(9):3599–3604. https://doi.org/10.1063/1.1681578

Mazeau K (2005) Structural micro-heterogeneities of crystalline iβ-cellulose. Cellulose 12:339–349. https://doi.org/10.1007/s10570-005-2200-5

Mazeau K, Heux L (2003) Molecular dynamics simulations of bulk native crystalline and amorphous structures of cellulose. J Phys Chem B 107(10):2394–2403. https://doi.org/10.1021/jp0219395

Mizuno M, Hirai A, Matsuzawa H, Endo K, Suhara M, Kenmotsu M, Han CD (2002) Study of odd- even effect of flexible spacer length on the chain dynamics of main-chain thermotropic liquid-crystalline polymers using high-resolution solid-state 13c nuclear magnetic resonance spectroscopy. Macromolecules 35(7):2595–2601. https://doi.org/10.1021/ma011839h

Mori T, Chikayama E, Tsuboi Y, Ishida N, Shisa N, Noritake Y, Moriya S, Kikuchi J (2012) Exploring the conformational space of amorphous cellulose using nmr chemical shifts. Carbohydr Polym 90(3):1197–1203. https://doi.org/10.1016/j.carbpol.2012.06.027

Nishiyama Y (2009) Structure and properties of the cellulose microfibril. J Wood Sci 55(4):241–249. https://doi.org/10.1007/s10086-009-1029-1

Nishiyama Y, Johnson GP, French AD, Forsyth VT, Langan P (2008) Neutron crystallography, molecular dynamics, and quantum mechanics studies of the nature of hydrogen bonding in cellulose iβ. Biomacromolecules 9(11):3133–3140. https://doi.org/10.1021/bm800726v

Nishiyama Y, Langan P, Chanzy H (2002) Crystal structure and hydrogen-bonding system in cellulose iβ from synchrotron x-ray and neutron fiber diffraction. J Am Chem Soc 124(31):9074–9082. https://doi.org/10.1021/ja025 7319

Nishiyama Y, Sugiyama J, Chanzy H, Langan P (2003) Crystal structure and hydrogen bonding system in cellulose iα from synchrotron x-ray and neutron fiber diffraction. J Am Chem Soc 125(47):14300–14306. https://doi.org/10.1021/ja037055w

Nishiyama Y, Wada M, Hanson BL, Langan P (2010) Time-resolved x-ray diffraction microprobe studies of the conversion of cellulose i to ethylenediamine-cellulose i. Cellulose 17:735–745. https://doi.org/10.1007/s10570-010-9415-9

Numata Y, Kono H, Kawano S, Erata T, Takai M (2003) Cross-polarization/magic-angle spinning 13c nuclear magnetic resonance study of cellulose i-ethylenediamine complex. J Biosci Bioeng 96(5):461–466. https://doi.org/10.1016/S1389-1723(03)70132-7

Pang Y, Jia D, Hu H, Hourston D, Song M (1999) A quantitative estimation of the extent of compatibilization in heterogeneous polymer blends using their heat capacity increment at the glass transition. J Appl Polym Sci 74(12):2868–2876

Parthasarathi R, Bellesia G, Chundawat S, Dale B, Langan P, Gnanakaran S (2011) Insights into hydrogen bonding and stacking interactions in cellulose. J Phys Chem A 115(49):14191–14202. https://doi.org/10.1021/jp203620x

Pinkert A, Marsh KN, Pang S, Staiger MP (2009) Ionic liquids and their interaction with cellulose. Chem Rev 109(12):6712–6728. https://doi.org/10.1021/cr9001947

Puiggalí J, Franco L, Alemán C, Subirana J (1998) Crystal structures of nylon 5, 6. a model with two hydrogen bond directions for nylons derived from odd diamines. Macromolecules 31(24):8540–8548. https://doi.org/10.1021/ma971895b

Reddy MM, Vivekanandhan S, Misra M, Bhatia SK, Mohanty AK (2013) Biobased plastics and bionanocomposites: Current status and future opportunities. Progr Polym Sci 38(10–11):1653–1689. https://doi.org/10.1016/j.progpolymsci.2013.05.006

Rios de Anda A, Fillot LA, Long DR, Sotta P (2016) Influence of the amorphous phase molecular mobility on impact and tensile properties of polyamide 6, 6. J Appl Polym Sci 133(21). https://doi.org/10.1002/app.43457

Rios de Anda A, Fillot LA, Preda F, Rossi S, Long D, Sotta P (2014) Sorption and plasticization effects of ethanol-toluene-isooctane ternary mixtures in polyamide 6, 6 and induced plasticization effects. Eur Polym J 55:199–209. https://doi.org/10.1016/j.eurpolymj.2014.04.001

Rios de Anda A, Fillot LA, Rossi S, Long D, Sotta P (2011) Influence of the sorption of polar and non-polar solvents on the glass transition temperature of polyamide 6, 6 amorphous phase. Polym Eng Sci 51(11):2129–2135. https://doi.org/10.1002/pen.22064

Schmidt-Rohr K, Spiess HW (eds) (2005) Multidimensional Solid-State NMR and Polymers. Academic Press, London

Schroeter J, Felix F (2005) Melting cellulose. Cellulose 12:159–165. https://doi.org/10.1007/s10570-004-0344-3

Segal L (1964) Comparison of the effects of allylamine and n-propylamine on cellulose. J Polym Sci Part A Gener Papers 2(6):2951–2961. https://doi.org/10.1002/pol.1964.100020643

Segal L, Eggerton F (1964) Study of the hexamethylenediamine-cellulose complex. J Polym Sci Part A Gener Papers 2(11):4845–4863. https://doi.org/10.1002/pol.1964.100021115

Segal L, Loeb L (1960) The diethylenetriamine-cellulose complex. J Polym Sci 42(140):351–356. https://doi.org/10.1002/pol.1960.1204214006

Sewda K, Maiti S (2013) Dynamic mechanical properties of high density polyethylene and teak wood flour composites. Polym Bull 70:2657–2674. https://doi.org/10.1007/s00289-013-0941-0

Su X, Kimura S, Wada M, Kuga S (2011) Stoichiometry and stability of cellulose-hydrazine complexes. Cellulose 18:531–537. https://doi.org/10.1007/s10570-011-9505-3

Thalladi VR, Boese R, Weiss HC (2000) The melting point alternation in alpha, omega-alkanediols and alpha, omega-alkanediamines: Interplay between hydrogen bonding and hydrophobic interactions the melting point alternation in n-alkanes and derivatives part 2. Angewandte Chemie 39(5):918–922

Uno K, Ogawa Y, Nakamura N (2008) Polymorphism of long-chain alkane-α, ω-diols with an even number of carbon atoms. Cryst Growth Des 8(2):592–599. https://doi.org/10.1021/cg700729q

VanderHart DL, Atalla R (1984) Studies of microstructure in native celluloses using solid-state carbon-13 nmr. Macromolecules 17(8):1465–1472. https://doi.org/10.1021/ma00138a009

Wada M, Heux L, Nishiyama Y, Langan P (2009) The structure of the complex of cellulose i with ethylenediamine by x-ray crystallography and cross-polarization/magic angle spinning 13 c nuclear magnetic resonance. Cellulose 16:943–957. https://doi.org/10.1007/s10570-009-9338-5

Wada M, Kwon GJ, Nishiyama Y (2008) Structure and thermal behavior of a cellulose i- ethylenediamine complex. Biomacromolecules 9(10):2898–2904. https://doi.org/10.1021/bm8006709

Wada M, Nishiyama Y, Bellesia G, Forsyth T, Gnanakaran S, Langan P (2011) Neutron crystallographic and molecular dynamics studies of the structure of ammonia-cellulose i: rearrangement of hydrogen bonding during the treatment of cellulose with ammonia. Cellulose 18:191–206. https://doi.org/10.1007/s10570-010-9488-5

Wada M, Okano T, Sugiyama J (2001) Allomorphs of native crystalline cellulose i evaluated by two equatoriald-spacings. J Wood Sci 47(2):124–128. https://doi.org/10.1007/BF00780560

Wang H, Gurau G, Rogers RD (2012a) Ionic liquid processing of cellulose. Chem Soc Rev 41(4):1519–1537. https://doi.org/10.1039/C2CS15311D

Wang Z, Liu S, Matsumoto Y, Kuga S (2012b) Cellulose gel and aerogel from licl/dmso solution. Cellulose 19:393–399. https://doi.org/10.1007/s10570-012-9651-2

Wickholm K, Larsson PT, Iversen T (1998) Assignment of non-crystalline forms in cellulose i by cp/mas 13c nmr spectroscopy. Carbohydr Res 312(3):123–129. https://doi.org/10.1016/S0008-6215(98)00236-5

Wormald P, Wickholm K, Larsson PT, Iversen T (1996) Conversions between ordered and disordered cellulose. effects of mechanical treatment followed by cyclic wetting and drying. Cellulose 3:141–152. https://doi.org/10.1007/BF02228797

Wu J, Bai J, Xue Z, Liao Y, Zhou X, Xie X (2015) Insight into glass transition of cellulose based on direct thermal processing after plasticization by ionic liquid. Cellulose 22:89–99. https://doi.org/10.1007/s10570-014-0502-1

Publisher's Note Springer Nature remains neutral with regard to jurisdictional claims in published maps and institutional affiliations.

Springer Nature or its licensor (e.g. a society or other partner) holds exclusive rights to this article under a publishing agreement with the author(s) or other rightsholder(s); author self-archiving of the accepted manuscript version of this article is solely governed by the terms of such publishing agreement and applicable law.